

Chitosan-Coated *Vitis vinifera L* Mediated Gold Nanoparticles for Controlled Released of Anticancer Drug Doxorubicin

Pradipta Das¹, Subash Das², Niranjana Rout³, Umesh Kumar Parida^{4*}

¹Department of General Surgery, KIMS, KIIT University, Bhubaneswar, Odisha, India

²Formulation and Development Product Unit, Kemwell Biopharma Pvt. Ltd. Bangalore, India

³Department of Onco-Pathology, A. H. Regional Cancer Centre, Cuttack, Odisha, India

⁴Newredmars Education Pvt. Ltd. Odisha, India

Received: 17th June, 17; Revised 27th August, 17, Accepted: 12th September, 7; Available Online: 25th September, 2017

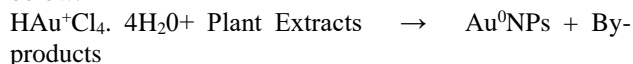
ABSTRACT

In this study, we developed encapsulating doxorubicin (DOX) drug loaded CS coated *Vitis vinifera L* mediated gold nanoparticles (V-AuNPs) [DOX loaded CS coated-V-AuNPs]. V-AuNPs were characterized by UV-Visible spectrophotometer, FTIR, XRD, TEM. The DOX-loaded CS coated-V-AuNPs was evaluated by particle size, surface charge, entrapment efficacy, and effect of pH in drug release profile. Additionally, drug entrapment efficacy (EE) was up to 56%; CS-DOX- V-AuNPs showed a pH-responsive drug release in vitro. The DOX release was nearly 84% at pH 5.4 and 67% at pH 7.4. The current work proves the potential of pharmacology that involves a fusion of advanced techniques from nanoscience to develop the biology and used in the fields of drug delivery, Bio Sensor Manufacturing, Medical therapy and the development of DOX-loaded CS coated-V-AuNPs nanoparticle for sustained, controlled release and may be useful for breast cancer treatment.

Keywords: *Vitis vinifera L*, AuNPs, Chitosan, Doxorubicin, Drug delivery

INTRODUCTION

During the past few decades, a variety of different methods have been reported and reviewed for synthesizing gold colloids of monodisperse and uniform sizes particles¹. Recently, the plant-mediated nanomaterial has drawn more attention due to its vast application in various biomedical fields due to their physicochemical properties²⁻⁸. The plant extract contains various type of biomolecules such as proteins, sugars, amino acids, enzymes and other traces of metals. These metabolites are strongly involved in the bioreduction process. The proposed reaction was Au⁺ ions reduction into metallic Au nanoparticles in the presence of metabolites and redox enzymes. The reaction is given below.



Last decade drug delivery system is a great challenge for pharmaceutical and medical science to the treatment of cancer disease. The newly emerging field of nanobiotechnology is gaining impotence owing to its wide application in drug designing and discovery field⁹. Gold nanoparticles possess unique physical, surface and chemical properties and are thus being used as carriers for the delivery of the drug^{10,11}. In the literature review, it has been reported that small size of AuNPs was cross-linking with Doxorubicin. Doxorubicin is an anti-cancer drug that has been shown to be more effectiveness when conjugated to hydrophilic nanoparticles that penetrate more deeply into the cell than the drug alone; nanoparticles may also

enhance uptake of unbound doxorubicin¹²⁻¹⁴. Additionally, Chitosan, the second abundant naturally occurring polysaccharide next to cellulose, is a biocompatible and biodegradable mucoadhesive polymer that has been extensively used for a potential carrier for different therapeutic agents such as peptides, proteins, vaccines, DNA, and drugs for parenteral and nonparenteral administration. Therapeutic Agent-loaded chitosan micro- or nanoparticles were found to be more stable, permeable, and bioactive¹⁵.

Grape consists in the skin, stems, and seeds of grapes that remain after processing in the wine and juice industry. Some other potential applications, such as the use of grape pomace to recover aroma compounds have been less explored. Some aromatic compounds can be present both as free volatiles and in much higher concentrations, as non-volatile sugar-bound glycoside conjugates. Despite the fact that grape glycosides are non-volatile odorless flavor precursors, under enzymatic or acid hydrolysis during winemaking they can release the corresponding odorant aglycones, which are generally potent flavor compounds (monoterpenes, norisoprenoids, benzenoids compounds, etc.) characterized by low aroma thresholds and interesting sensory properties^{16,17}.

In this work, our idea here was to develop an innovative strategy for DOX-loaded CS coated-V-AuNPs to perform enhance the effectiveness of DOX, to overcome DOX resistance and to reduce the toxicity associated and also study its entrap and release, in a controlled manner.

MATERIAL AND METHOD

Chemicals and Plant Material

Tetrachloro auric acid ($\text{HAuCl}_4 \cdot \text{XH}_2\text{O}$) was purchased from Sigma-Aldrich. Chitosan and Doxorubicin were purchased from Himedia and Sigma-Aldrich. All other chemicals were used as an analytical grade. Millipore Water was used in the entire experimental work. The *vitis vinifera* L fruit was purchased from local market Bhubaneswar Odisha, India.

Preparation of Fruit Extract

The Fresh *vitis vinifera* L fruit (V) was collected from the local market (Bhubaneswar, Odisha, India). Mature fruits were washed and extract prepared with triple distilled water. The extract was centrifuged at 2,000 rpm for 10 minutes. The supernatant containing the extract was filtered through 0.2 μm syringe filter (EMD Millipore) and collected in separate conical flasks by standard filtration method and stored at 4°C.

Synthesizing the V-AuNPs

AuNPs were synthesized by the reduction of $\text{HAuCl}_4 \cdot \text{XH}_2\text{O}$ by *V. vinifera* L. fruit extracts. 50 ml of triple distilled water was heated to 60°C in a boiling flask, followed by the addition of 500 μL of *V. vinifera* L. fruit extract with constant stirring for 10 minutes. Then, 500 μL (0.1 M HAuCl_4) was added dropwise to the mixture. The color of the reaction mixture changed to purple pink, indicating the synthesis of V-AuNPs. The reaction was stopped by immediate cooling on ice. V-AuNPs with different sizes were obtained by changing the reaction parameters¹⁸.

Chitosan-coated V-AuNPs

The chitosan of 1gm is made solubilised in 1% acetic acid of 50ml by mixing and heating at 45°C by stirring. To the above solution was added V-AuNPs in 1:3 ratio and continuing constant stirring without heat supplied for 2 hours. Then prepared CS coated V-AuNPs were ready for further processing¹⁹.

DOX loading in CS coated V-AuNPs

DOX-loaded CS coated V-AuNPs nanoparticles (1 mg/mL) were mixed and incubated on a magnetic stirrer at 800 rpm overnight. Free CS particles were removed by centrifugation at 4000 rpm for 10 minutes. The DOX-loaded CS coated V-AuNPs nanoparticles were collected by ultra-centrifugation at 30000 rpm for 15 minutes at 4 °C. Based on the above preparation of DOX-loaded CS coated V-AuNPs, we have drawn a scheme of the mechanism of action for CS coated V-AuNPs for controlled drug released (Figure 1).

Characterization of NPs

UV-visible spectral analysis

The UV-visible spectrum from 200 to 900 nm of fruit extract, CS, V-AuNPs, CS coated V-AuNPs and DOX-loaded CS coated V-AuNPs with different pH medium were recorded in an EPOCH™ Multi-Volume Spectrophotometer System (Biotek Instruments, Inc., Mumbai, India). V-AuNPs displayed maximum absorbance at 535 nm with predominance of smaller size particles²⁰.

X-ray diffraction analysis (XRD)

The lyophilized powders of the V-AuNPs were used for XRD study (powder X-ray diffractometer, Bruker, USA). The diffracted intensities were reported from 0 to 80° at 2 θ angles. The diffraction pattern corresponds to CS, V-AuNPs, CS coated V-AuNPs, and DOX-loaded CS coated V-AuNPs. The received results illustrate that HAuCl_4 had indeed been reduced to form of V-AuNPs by *vitis vinifera* fruit extract under reaction conditions²⁰.

Fourier transforms infrared spectral studies (FTIR)

To examine the chemical functional group interactions between the *V. vinifera* fruit extract, CS, V-AuNPs, DOX, CS coated V-AuNPs and DOX-loaded CS coated V-AuNPs, FTIR spectra study was taken out using a PerkinElmer Model Spectrum 1 (PerkinElmer, MA, USA). An FTIR spectrum was examined in the range between 500 and 4000 cm^{-1} .

Transmission electron microscopy (TEM)

Morphological characterization of V-AuNPs was carried out by TEM (JEOL-JEM 2100, 1.4 Angstrom Unit, Tokyo, Japan). The V-AuNP and DOX-loaded CS coated V-AuNPs was made by air-drying drops of diluted V-AuNP solutions on carbon films supported by copper grids. TEM images were visualized at 120 kV under the microscope.

Particle size analysis & zeta-potential measurements

Dynamic light scattering (DLS) was used to estimate the hydrodynamic diameter, and laser Doppler anemometry was used to determine zeta-potential (mV). The DLS and laser Doppler anemometry analyses were shown using a Zetasizer Nano ZS (Malvern Instruments, Worcestershire, UK). To define the particle size and zeta-potential, a dilute suspension of V-AuNPs (100 μl diluted to 1 ml Milli-Q water) was sonicated in an ice bath for the 30s and subjected to particle size and zeta potential determination.

Entrapment Efficiency and Drug Content

During the preparation of DOX encapsulated in CS coated V-AuNPs, the amount of DOX encapsulated into the nanoparticles was calculated by EE formula. A calibration curve was developed using the known standard concentrations of DOX dissolved in DI water. The spectrophotometric quantification was achieved by taking the absorbance at 254 nm. The EE was calculated using the following formula:

$$EE\% = \frac{\text{Total amount of DOX used} - \text{amount of DOX in the CS coated V - AuNPs}}{\text{Total amount of drug used}} \times 100$$

Then, percentage of DOX content in Cs coated V-AuNPs

$$\text{DOX drug loading} = \frac{L}{L_0} \times 100$$

DOX release from CS coated V-AuNPs-DOX

To analysis, DOX from CS-V-AuNPs, 50 mg of each formulation was incubated in 5 ml of 1x PBS at pH 7 at room temperature. At different time intervals, 5 ml of the supernatant was withdrawn and followed with fresh buffer. Additionally, measurement of effect pH on DOX release from CS coated V-AuNPs, two different buffer solutions: 1X PBS pH 7.4 (physiological pH) and pH 5.4 (pH of tumor tissue) were used to study the effect of pH on drug release. The absorbance of each solution was calibrated by

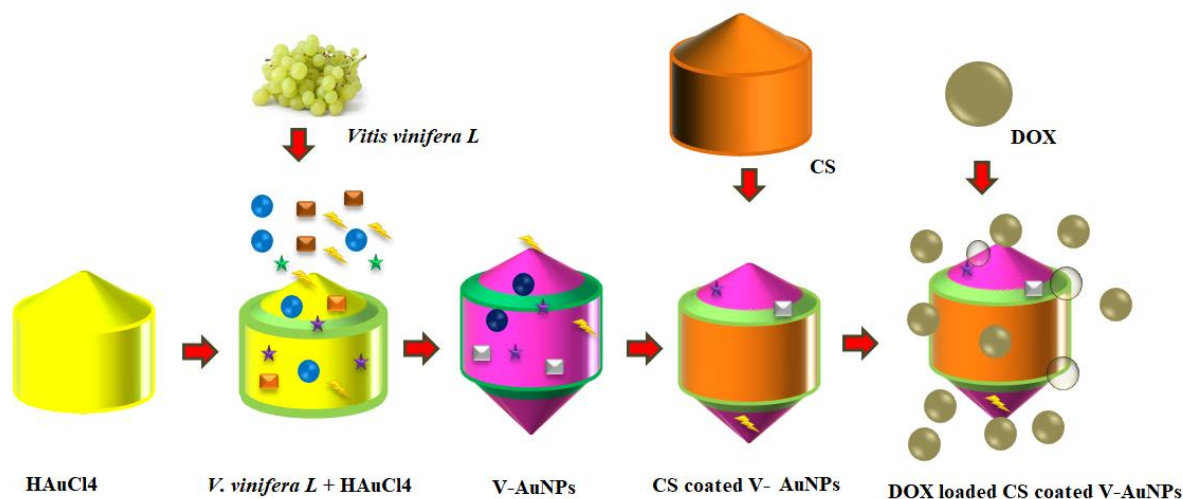


Figure 1: schematically presented DOX-loaded CS coated V-AuNPs nanoparticles.

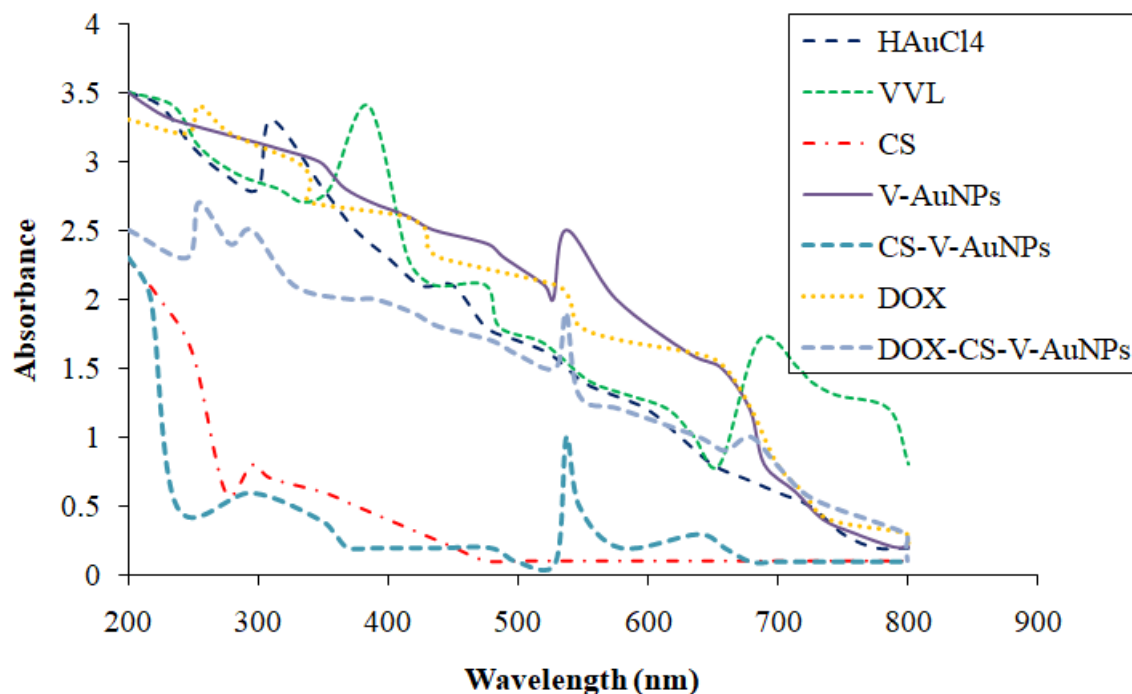


Figure 2: UV–AuNPs, DOX-loaded CS coated V-AuNPs in water visible spectrum of HAuCl₄ solution, CS, fruit extract solution, DOX, V-

using a UV-Spectrophotometer at a wavelength of 254 nm. All experiments were presented in triplicate.

Statistical analysis

Data were expressed as mean \pm SD or SEM. Statistical analysis was done by one-way ANOVA where appropriate with Graph Pad Prism 5.0 (Graph Pad Software Inc., San Diego, CA, USA).

RESULTS

UV-Vis Spectroscopic

Figure 2 shows the UV-visible absorption spectrum of the HAuCl₄ solution, CS, *V. vinifera L* fruit extract (VVL), DOX, V-AuNPs, CS coated V-AuNPs, DOX-loaded CS coated V-AuNPs in water. The UV-visible

spectrophotometer analysis of the product obtained displayed peaks and bands for SPR absorption. It was observed that the optimum reaction mixture SPR absorbance peak at 535 nm which is also clearly observed in CS coated V-AuNPs in water. The stability of the V-AuNPs and CS coated V-AuNPs-DOX was determined by measuring the absorption spectrum at 24-h intervals for 90 days. No significant changes in absorbance were determined during storage time at 37°C, indicating that the V-AuNPs were stable during this period¹⁸.

XRD

In Figure 3, the XRD pattern of the HAuCl₄ solution, CS, VVL, DOX, V-AuNPs, DOX-loaded CS coated V-AuNPs are explained. The diffraction peaks for CS coated V-

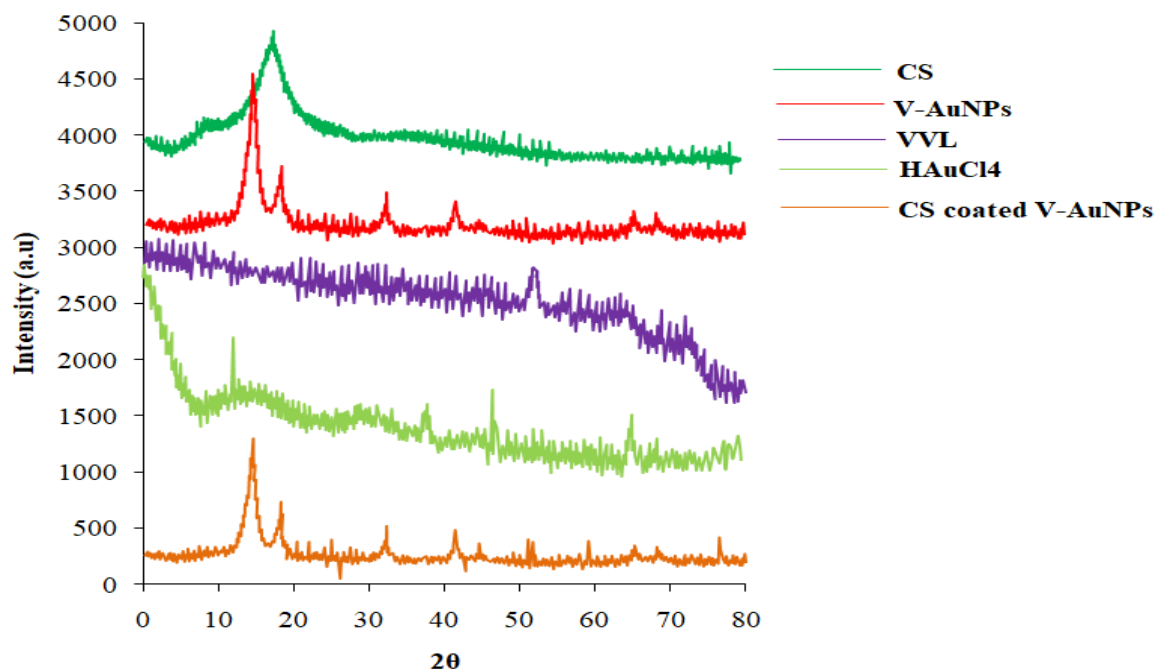


Figure 3: X-ray diffraction analysis of HAuCl₄ solution, CS, VVL, DOX, V-AuNPs, CS coated V-AuNPs, and DOX-loaded CS coated V-AuNPs.

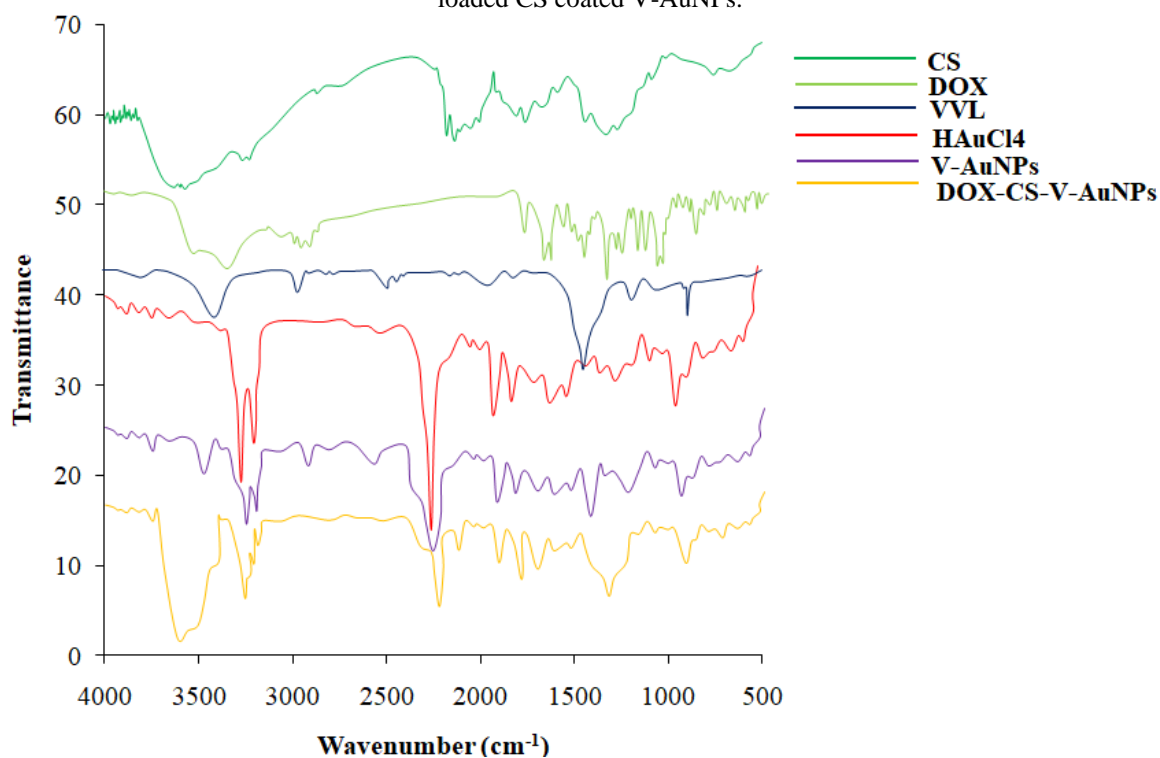


Figure 4: Fourier transform infrared spectra of HAuCl₄ solution, CS, fruit extract solution, DOX, V-AuNPs, DOX-loaded CS coated V-AuNPs.

AuNPs was found at 19, 45 and 57°, which is different from CS, VVL and V-AuNPs with higher in intensity. The result was manipulated to study the crystal structure of V-AuNPs, and CS coated V-AuNPs. The specific X-Ray diffraction pattern of the V-AuNPs obtained from green rour was obtained by Bragg reflections corresponding to the (111), (200), (220), (311) and (222) sets of lattice

planes are observed that may be indexed by the fcc structure of V-AuNPs.

FTIR

Figure .4 presents the FTIR spectra of the HAuCl₄ solution, CS, VVL, DOX, V-AuNPs, CS coated V-AuNPs, and DOX-loaded CS coated V-AuNPs. VVL contains mainly glucose, fructose, sugar, peptides, proteins tartaric, nitrogenous compound amino acid, anthocyanins organic

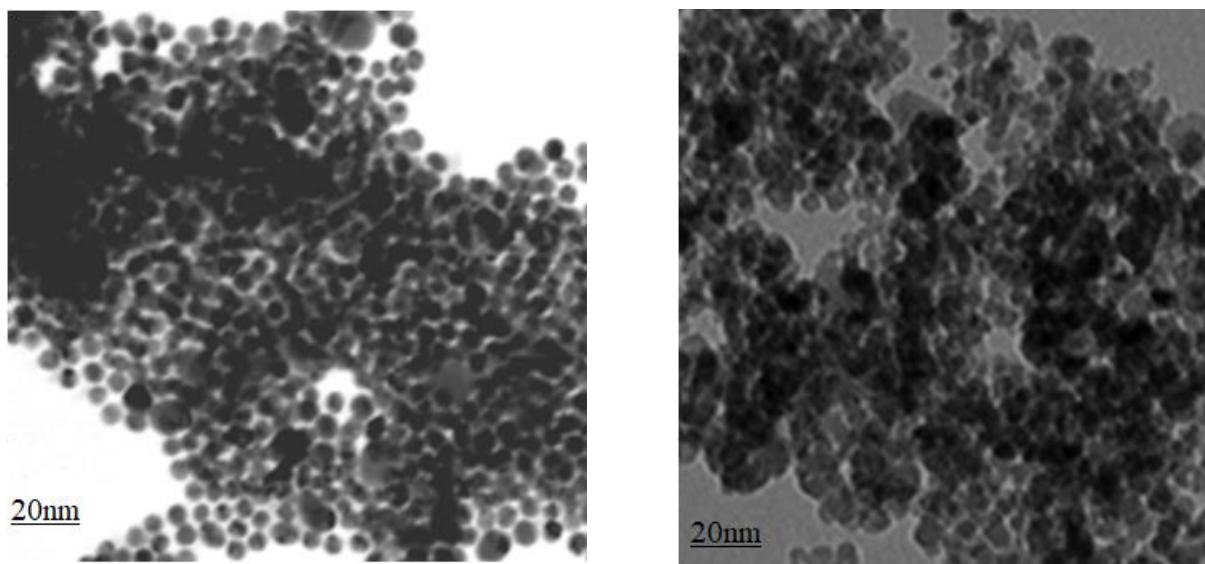


Figure 5: TEM and DLS of a: V-AuNPs and b: CS coated V-AuNPs.

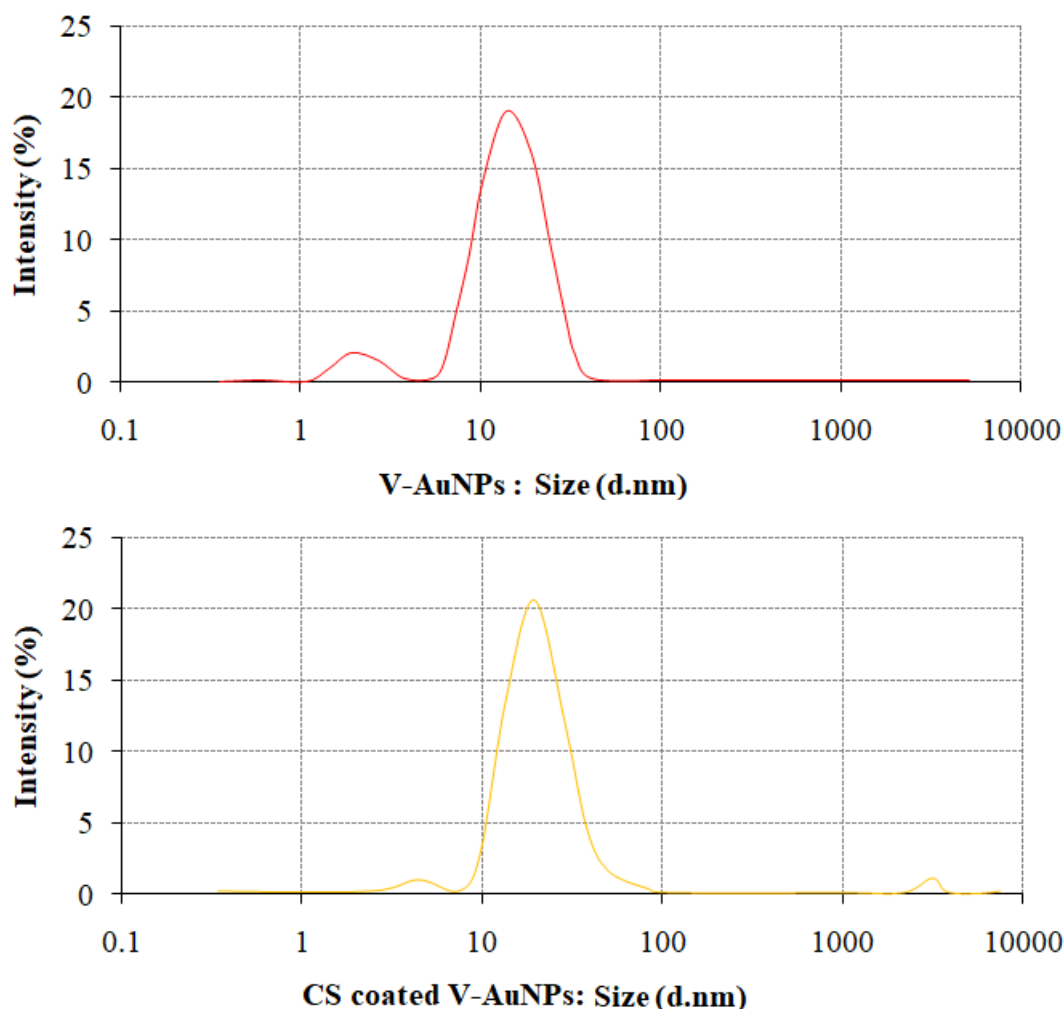


Figure 6: DLS of a: V-AuNPs, b: CS coated V-AuNPs.

acid, citric acid and phenolic compounds²¹. In the characteristic peaks seen for V-AuNPs peak at 3683 cm^{-1} was probably an O-H stretch, 2825 cm^{-1} , and 2121 cm^{-1} indicate the C-H and C≡H of alkanes and alkynes, 2801 cm^{-1} and 2798 cm^{-1} are indicative of C-H and H-C=O bonds of aldehydes, 1592 cm^{-1} and 1589 cm^{-1} are

indicative of N-H bond vibrations from amide groups of the proteins present in VVL extract as well as in the V-AuNPs¹⁸. By contrast, some peaks were shifted in sample CS coated V-AuNPs and DOX-loaded CS coated V-AuNPs comparing with V-AuNPs, CS, DOX, VVL. It was clear that VVL extract, CS, and DOX had been

Table 1: Zeta-potential of a: V-AuNPs, b: DOX-loaded CS coated N-AuNPs.

Sample	Zeta potential	DLS
V-AuNPs	2.251 ± 4.1	25 ± 2nm
CS-AuNPs	2.468 ± 4.3	29 ± 1nm

Table 2: Kinetic study of in vitro drug release data from CS coated DOX loaded V-AuNPs

Release model		CS-DOX-V-AuNPs
Zero Order	R ²	0.8932
	k	0.2611
First Order	R ²	0.9742
	k	0.0832
Higuchi Matrix	R ²	0.9725
	k	0.0935
Peppas	R ²	0.9954
	k	1.1126
	n	0.7321

synthesized, coated and encapsulated on the surface of V-AuNPs and formed the chemical bond with V-AuNPs.

DLS

TEM was presented on the V-AuNP and CS coated V-AuNPs, to visualize the morphology of nanoparticles. The images were shown that particles are spherical and polydispersed with a size ranging from 10 to 30 nm in (figure 5a and b). Next, DLS analysis exhibited that the formulated V-AuNP and DOX-loaded CS coated V-AuNP had an average diameter of 16.2 ± 1.4 nm and 28.4 ± 1.2 nm (figures 6a and b).

Zeta-potential

The data in table.1 shows the zeta-potential to be positive, with a value of 2.251 ± 4.1 mV of V-AuNP and 2.468 ± 4.7 mV of CS coated V-AuNPs. The neutral CS effectively coats the positively charged surface of the V-AuNPs, but the particles retain their positively charged characteristic. This data proves that the DOX-loaded CS coated V-AuNPs are homogeneously coated.

Effect of pH on Drug release

The pH dependent in vitro drug release from DOX-loaded CS coated V-AuNPs was carried out in different buffered solution with pH 7.4 (physiological pH) and 5.4 (similar to tumor tissue pH) at 37°C. Figure 7 shows initial sustained release of DOX from CS coated V-AuNPs. Figure 7 shows highly different DOX release profile from CS coated V-AuNPs in same pH condition about 67% for pH 7.4 and 84% for pH 6.5. It also seen both release profiles exhibited rapid burst effect during the first 7 to 8 h. This result was suggested that pH independent nature of the Sample.

The data from the in vitro release studies was subjected to kinetic analysis, that is, zero-order and first-order. To determine the mechanism that best represented the release of the drug from the formulations, the data was also fitted to the Higuchi matrix model and Korsmeyer–Peppas equation. The release exponent (n) describing the mechanism of drug release from the matrices was calculated by regression analysis, using the Peppas equation²².

$$M_t / M_\infty = k t^n$$

Where M_t / M_∞ is the fraction of drug released (using values of M / M_∞) at time t , and k is a constant incorporating the structural and geometric properties of the release device. When $n = 0.5$, Case I or Fickian diffusion is indicated, $0.5 < n < 1$ for anomalous (not-Fickian) diffusion, $n = 1$ for Case II transport (Zero order release), and $n > 1$ indicates (Costa and Sousa Lobo 2001). The experimental research data of k , n , and R^2 (coefficient of determination) have been obtained using the PCP Disso V 2.08 software as presented in Table 2.

The values of n obtained by the linear regression of $\log(M_t / M_\infty)$ versus $\log t$, were between 0.5 to 1 for all formulations, indicating non-fickian diffusion as the release mechanism, and close to 0.5 in the case of DOX-CS coated V-AuNPs, to follow first order kinetics. Peppas model was the best, and highest R^2 for DOX-CS coated V-AuNPs, the results of R^2 for the Higuchi matrix model and First order model for DOX-CS coated V-AuNPs was greater than Zero order model, indicating matrix-diffusion controlled release from the hydrophilic polymer matrices by first order kinetics.

DISCUSSION

Several lines of evidence suggest that AuNPs have a wide variety of applications in diverse fields, including cancer chemotherapy. Recently, investigators reported that AuNPs are capable of drug delivery agent in vivo and in vitro^{10,23-25}. However, there is a lack of literature regarding the use of AuNPs as drug delivery carrier against cancer cells. Moreover, the detailed green synthesis of AuNPs for biochemical mechanisms and drug delivery activities were not known. In the present report, we have shown for the first time that CS coated V-AuNPs exhibit controlled drug release using anticancer drug doxorubicin. This study has systematically established the green synthesis, and drug delivery applications of *V. vinifera* L. fruit extract mediated V-AuNPs coated by chitosan.

For this study, we prepared a stable, purified form of V-AuNP using *V. vinifera* L. fruit extract as a reducing agent, which showed remarkable stability and uniform distribution throughout the test period without any sign of aggregation and precipitation (Figure 2). In physicochemical characterization of the V-AuNPs revealed the excellent average size, and uniform surface charge analyzed in figure.3 to figure.6 and table-1. The *V. vinifera* L. extract alone could reduce HAuCl_4 salt to produce V-AuNPs, but these V-AuNPs were not stable and formed aggregates on long-term storage. Therefore, CS was used as a stabilizer to avoid aggregation of V-AuNPs. CS is a highly branched polysaccharide structure. The potential adverse effects of nanomaterials on human health are expected to reduce to a greater extent with the use of V-AuNPs synthesized from natural plant compounds, such as polyphenols and phytochemicals, that are known to have abundant antioxidant and anticancer properties^{26,27}. In the current method, the organic acids, phenolic compounds, and polysaccharides might have reduced the NaAuCl_4 into the GNPs.

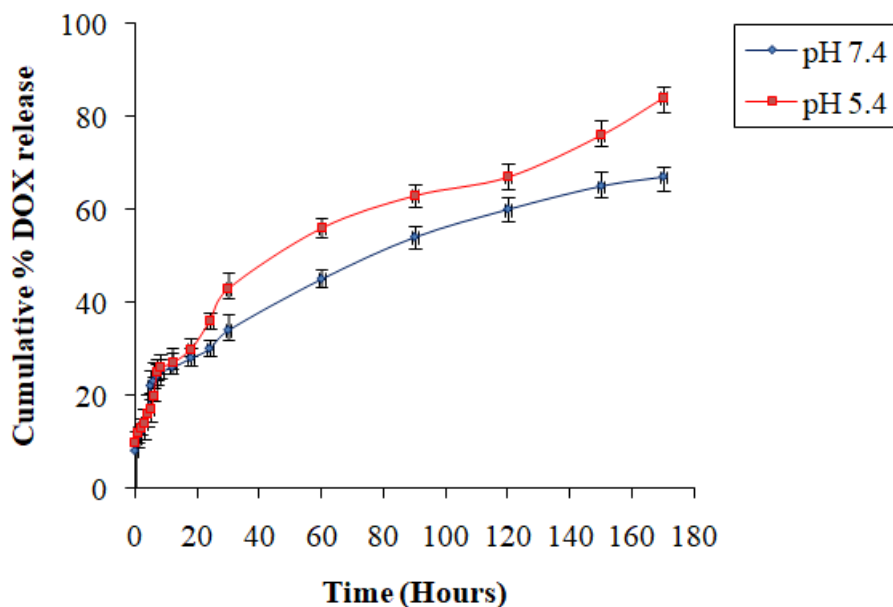


Figure 7: Effect of different pH (5.4 and 7.4) on CS coated V-AuNPs nanocarrier for controlled drug release of DOX at 37°C (means; n=3), Kinetic analysis of in vitro release data.

Anticancer drug delivery has focused on discovering and developing drugs that target a single protein on the cancer cell. However, there is currently an increasing demand on chitosan has been extensively used as a potential carrier for different therapeutic agents¹⁵. In this study, CS coated V-AuNPs was shown a good drug delivery carrier for controlled drug released of anticancer drug DOX. The pH dependent in vitro drug release from CS coated V-AuNPs was demonstrated that DOX was very good release in the acidic medium than basic medium in figure 7. Peppas model was the best, and highest R² for DOX-CS coated V-AuNPs and Higuchi matrix model, and first order model for DOX-CS coated V-AuNPs was greater than Zero order model in table-2.

The prepared V-AuNPs used here were synthesized by a simple green synthesis procedure that is also environmentally friendly and cost effective. A better understanding of the bioactivity and drug delivery nature of CS coated V-AuNP will speed their entry into clinical trials

CONCLUSION

The study involved the green method for the production of V-AuNPs is the reduction of the carboxylic acid groups. The work also describes the synthesis and surface functionalization of V-AuNPs, CS coated V-AuNPs, and DOX-CS coated V-AuNPs. The results of the V-AuNPs synthesis and their functionalization were checked by using XRD, FTIR, TEM, DLS, and UV/Vis spectroscopy techniques. The resulting V-AuNPs are hydrophilic and show little aggregation, even when conjugated to somewhat hydrophobic molecules such as doxorubicin. This is significant because the hydrophobicity of many anti-cancer drugs is a barrier to their effective use. As a result, many encapsulated and conjugated nanoparticle preparations have been prepared. A new strategy of the

DOX-CS coated V-AuNPs was successfully synthesized by green synthesis method. The data and the promises shown by the DOX-CS coated V-AuNPs nanoparticles in our preclinical study indicate the high efficiency of this formulation for further translation into clinics.

REFERENCE

1. Rochelle R.A, Bhattacharyya S , Rachel K, Giri K, Bhattacharya R , and Mukherjee P. Intrinsic Therapeutic Applications of Noble Metal Nanoparticles: Past, Present and Future. *Chem Soc Rev.* 2012; 41(7): 2943–2970.
2. Ahmad B, Nabia H, Bashir S, Rauf A. Phytofabricated gold nanoparticles and their biomedical applications. *Biomedicine & Pharmacotherapy* 2017;89, 414-425.
3. Cornejo-Monroy D, Acosta-Torres LS, Moreno-Vega AI, Saldana C, Morales-Tlalpan V, Castaño VM. Gold nanostructures in medicine: past, present and future. *J Nanosci Lett.* 2013;3:25.
4. Elia P, Zach R, Hazan S, Kolusheva S, Porat Z. Green synthesis of gold nanoparticles using plant extracts as reducing agents *Int J Nanomedicine.* 2014; 9: 4007–4021.
5. Khan Z, Khan A, Chen Y, Shah N.S., Muhammad N, Khan A.U, Tahir K, Khan F. U, Murtaza B, Hassan S.U, Qaisrani S.A, Wan P. Biomedical applications of green synthesized Nobel metal nanoparticles. *Journal of Photochemistry and Photobiology B: Biology,* 2017;173: 150-164.
6. Zheng Y, Lai L, Liu W, Jiang H, Wang X, Recent advances in biomedical applications of fluorescent gold nanoclusters. *Advances in Colloid and Interface Science,* 2017;242:1-16.
7. Shi W, Sahoo Y, Swihart MT. Gold nanoparticles surface-terminated with bifunctional ligands. *Colloids Surf A Physicochem Eng Asp.* 2004;246(1):109–113.

8. Kumar KM, Mandal BK, Sinha M, Krishnakumar V. Terminalia chebula mediated green and rapid synthesis of gold nanoparticles. *Spectrochim Acta A Mol Biomol Spectrosc.* 2012;86:490–494.
9. Haley B, Frenkel E. Nanoparticles for drug delivery in cancer treatment. *Urol Oncol.* 2008;26(1):57-64.
10. Erik C Dreaden, Lauren A Austin, Megan A Mackey, and Mostafa A El-Sayed. Size matters: gold nanoparticles in targeted cancer drug delivery, *Ther Deliv.* 2012 ; 3(4): 457–478.
11. Ghosh P, Han G, De M, Kim C.K. Gold nanoparticles in delivery applications, *Advanced Drug Delivery Reviews.*2008; 60(11):1307-1315.
12. Tomuleasa C, Soritau O, Orza A, Dudea M, Petrushev B, Mosteanu O, Susman S, Florea A, Pall E, Aldea M, Kacso G, Cristea V, Berindan-Neagoe I, Irimie A. Gold nanoparticles conjugated with cisplatin/doxorubicin/capecitabine lower the chemoresistance of hepatocellular carcinoma-derived cancer cells. *J Gastrointestin Liver Dis.* 2012;21(2):187-96.
13. Madhusudhan A, Reddy G. B, Venkatesham M, Veerabhadram G, Kumar D.A, Natarajan S, Yang M. Y, Hu A, Singh S.S. Efficient pH Dependent Drug Delivery to Target Cancer Cells by Gold Nanoparticles Capped with Carboxymethyl Chitosan *Int J Mol Sci.* 2014; 15(5): 8216–8234.
14. Amreddy N, Muralidharan R, Babu A, Mehta M, Johnson E.V, Zhao Y.D, Munshi A, Ramesh R, Tumor-targeted and pH-controlled delivery of doxorubicin using gold nanorods for lung cancer therapy *Int J Nanomedicine.* 2015; 10: 6773–6788.
15. Ahmed T. A, Aljaeid B.M. Preparation, characterization, and potential application of chitosan, chitosan derivatives, and chitosan metal nanoparticles in pharmaceutical drug delivery. *Drug Des Devel Ther.* 2016; 10: 483–507.
16. Liang Z, Cheng L, Zhong G.Y, Liu R.H. Antioxidant and Antiproliferative Activities of Twenty-Four *Vitis vinifera* Grapes . *PLoS One.* 2014; 9(8): e105146.
17. Garavaglia J, Markoski M.M., Oliveira A, Marcadenti A. Grape Seed Oil Compounds: Biological and Chemical Actions for Health *Nutr Metab Insights.* 2016; 9: 59–64.
18. Kalmodia S , Harjwani J , Rajeswari R , Yang W , Barrow C. J , Ramaprabhu S , Krishnakumar S , and Sailaja V. E. Synthesis and characterization of surface-enhanced Raman-scattered gold nanoparticles. *Int J Nanomedicine.* 2013; 8: 4327–4338.
19. Sun IC, Na JH, Jeong SY, Kim DE, Kwon IC, Choi K, Ahn CH, Kim K. Biocompatible glycol chitosan-coated gold nanoparticles for tumor-targeting CT imaging. *Pharm Res.* 2014; 31(6):1418-25.
20. Rout Anandini, Jena Padan K., Sahoo Debasish , Parida Umesh K. and Bindhani B. K., Green Synthesis and Characterization of Silver Nanoparticles for Antimicrobial Activity Against Burn Wounds Contaminating Bacteria, *International Journal of Nanoscience* 2014; 13(2):1450010.
21. Xia EQ, Deng GF, Guo YJ, Li HB. Biological activities of polyphenols from grapes. *Int J Mol Sci.* 2010;11:622–646.
22. Peppas NA. Analysis of Fickian and non Fickian drug release from polymers. *Pharm Acta Helv* 1985;60:110-1.
23. Gu Y-J, Cheng J, Man CW-Y, Wong W-T, Cheng SH. Gold-doxorubicin nanoconjugates for overcoming multidrug resistance. *Nanomedicine.* 2011;8(2):204–211.
24. Cheng Y, C. Samia A, Meyers JD, Panagopoulos I, Fei B, Burda C. Highly efficient drug delivery with gold nanoparticle vectors for in vivo photodynamic therapy of cancer. *J. Am. Chem. Soc.* 2008;130(32):10643–10647.
25. Bergen JM, Von Recum HA, Goodman TT, Massey AP, Pun SH. Gold nanoparticles as a versatile platform for optimizing physicochemical parameters for targeted drug delivery. *Macromol. Biosci.* 2006;6(7):506–516.
26. Visioli F, De La Lastra CA, Andres-Lacueva C, et al. Polyphenols and human health: a prospectus. *Crit Rev Food Sci Nutr.* 2011;51:524–546.
27. Russo M, Spagnuolo C, Tedesco I, Russo GL. Phytochemicals in cancer prevention and therapy: truth or dare? *Toxins (Basel)* 2010;2:517–551.